Medical Engineering and Physics 64 (2019) 56–64

Contents lists available at ScienceDirect

Medical Engineering and Physics

journal homepage: www.elsevier.com/locate/medengphy

Same day cerebral perfusion and dopamine transporter imaging for differential diagnosis of cerebral impairment☆

Thomas J. Biggans

Nuclear Medicine, Ninewells Hospital, Dundee, DD1 9SY, United Kingdom

ARTICLE INFO

Article history:
Received 22 December 2017
Revised 17 December 2018
Accepted 31 December 2018

Keywords:
Brain SPECT imaging
DaTscan
FP-CIT
HMPAO
Dual isotope
Crosstalk compensation
Parkinson's
Lewy body dementia

ABSTRACT

When cognitive impairment is first evident it can be difficult to distinguish between different conditions such as idiopathic Parkinson's disease and Lewy body dementia. Imaging both cerebral perfusion and dopamine transporter function has been shown to provide accurate differentiation between the most common conditions. At present cerebral perfusion and dopamine transporter imaging is conducted on separate days. Carrying out both scans on the same day has the potential to benefit the patient through the social convenience of one visit to hospital and the earlier availability of results.

This work considered whether it was possible to obtain diagnostic quality images from Ioflupane (^{123}I) single positron emission tomography (SPECT) acquired at the same time as or four hours after a Exametazime (^{99m}Tc) SPECT on the same day. Possible changes to the Ioflupane (^{123}I) SPECT acquisition and processing protocols such as a new energy window and use of a resolution recovery algorithm were explored using phantom studies.

Initial phantom results show that when a four hour delay between acquisitions is used comparable contrast to noise ratios can be achieved (4.23 vs. 4.63) with an insignificant loss in resolution (11.51 mm vs. 11.35 mm full width at half maximum (FWHM)). An offset energy window (159 keV −5.5% & +15.5%) was found to provide the highest contrast to noise ratio. This work provides a proof of concept for same day imaging.

1. Introduction

When cognitive impairment is first evident it can be difficult to distinguish between different conditions, such as idiopathic Parkinson's disease and Lewy body dementia, which exhibit shared symptoms such as rigidity, tremor, issues with speech or gait disturbance [1]. When Lewy body dementia is suspected, imaging both cerebral perfusion and dopamine transporter function can eliminate other possible conditions (idiopathic Parkinson's disease, cerebral vascular disease, Alzheimer's disease or frontotemporal dementia) [2].

At present perfusion and dopamine transporter imaging are usually conducted on separate days possibly weeks apart. Simultaneous imaging is challenging due to the close proximity of the photon energies emitted from ^{99m}Tc (140 keV) and ^{123}I (159 keV) (Fig. 1). It is difficult to separate the perfusion image (^{99m}Tc) from the dopamine transporter image (^{123}I) resulting in two sets of poor quality images. The overlap of the two energies (crosstalk) is a result of the energy resolution on conventional gamma cameras (approximately 9%) [3].

A great deal of work has been undertaken to compensate for dual-isotope crosstalk during simultaneous acquisitions [4–6]. These methods, which include artificial intelligence and Monte Carlo modelling, usually involve complex post acquisition processing which can be difficult to implement in a clinical setting. This work considered whether it was possible to obtain diagnostic quality images, using more conventional techniques, from Ioflupane (^{123}I) (DaTscan, GE Healthcare, Waukesha, WI, USA) SPECT acquired four hours after Exametazime (^{99m}Tc) (Ceretec, GE Healthcare, Waukesha, WI, USA) SPECT (delay protocol).

Acquiring both sets of images on the same day can be more convenient for the patient than the current arrangement of separate appointments. Furthermore, in the case of the same day protocol, the Exametazime (^{99m}Tc) (also known as HMPAO) SPECT acquisition would be conducted independently so the quality of the cerebral perfusion images would be unaffected.

Locally the administered activities used are 500 and 185 MBq for Exametazime (^{99m}Tc) and Ioflupane (^{123}I), respectively. This

☆ The peer review of this manuscript was overseen by Guest Editor Stephen Keevil. The paper is based on work that was presented at the Joint Annual Conference of IPEM and the Bioengineering Society: MEIBioeng/MPEC, Sandown Park, London, 13-14 September, 2017 https://www.ipem.ac.uk/ConferencesEvents/MPECMEIbioeng2017.aspx.

E-mail address: thomas.biggans@nhs.net

https://doi.org/10.1016/j.medengphy.2018.12.016
1350-4533/

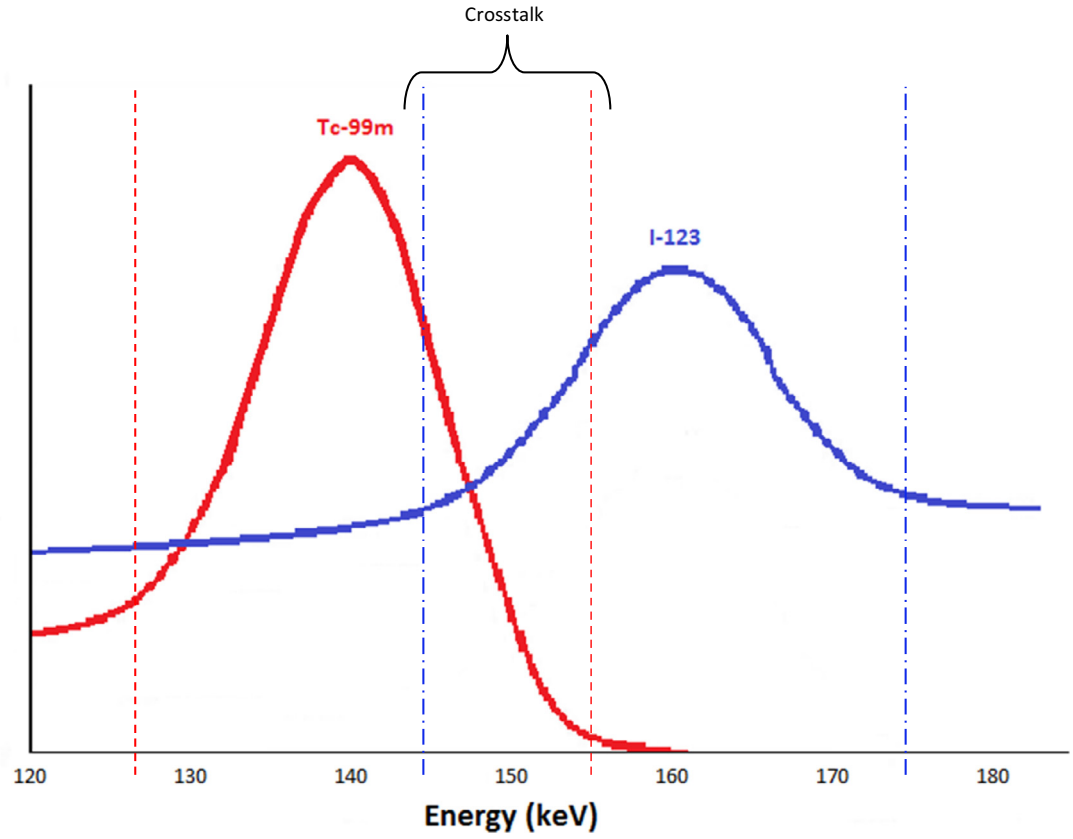

Fig. 1. Energy spectrums of Tc-99 m and I-123 gamma photons. Standard energy window boundaries are indicated by dashed lines.

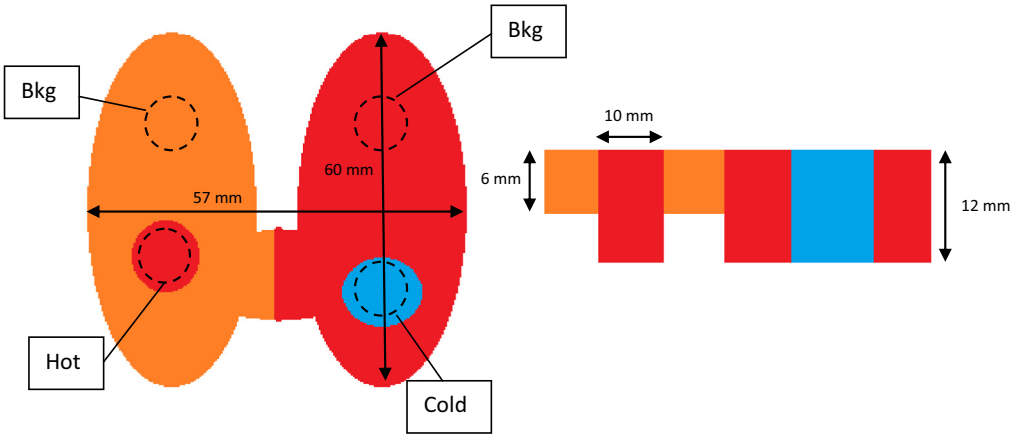

Fig. 2. Schematic of bespoke phantom. Areas in red are twice the depth of the areas in orange. The blue area is solid Perspex and does not contain any activity. (For interpretation of the references to color in this figure legend, the reader is referred to the web version of this article.)

corresponds to an average adult effective dose of 4.7 mSv from ^{99m}Tc and 4.6 mSv from ^{123}I with the patient's thyroid blocked [7]. This work assumed that the administered activity of each isotope would not be changed. Therefore the total dose to the patient and the amount of waste generated would also be the same. There may be a small increase in the instantaneous external dose rate from the patient by following the one day protocol but it is reasonable to conclude that overall the total dose to all involved would be similar to the current practice.

2. Methods

Phantom studies were performed using a GE Discovery NM/CT 670 dual-head gamma camera (GE Healthcare, Waukesha, WI, USA) with an intrinsic energy resolution of 9.2% FWHM. Acquisitions were conducted with Low Energy High Resolution (LEHR) and Extended Low Energy General Purpose (ELEGP) parallel hole collimators. Initially a planar setup was used to evaluate various acquisition options. Using the planar results as a guide, SPECT data was acquired for the preferred option.

2.1. Planar

Planar data was acquired in a 256 × 256 matrix with an acquisition time of 5 min and no zoom. A camera to phantom distance of 15 cm was used throughout. A bespoke Perspex phantom was used as a suitable analogue to the basal ganglia. The phantom (Fig. 2) used differing depths to create contrast on planar images. It was filled with 378 kBq/mL (^{123}I) sodium iodide diluted in water. This

Table 1
Collimator and energy window combinations for planar phantom studies.

Planar acquisition method	Phantom setup	Collimator	Energy window
ELEGP reference	^{123}I only	ELEGP	159 keV −10% & +10%
ELEGP normal	^{123}I with ^{99m}Tc background	ELEGP	159 keV −10% & +10%
ELEGP narrow	^{123}I with ^{99m}Tc background	ELEGP	159 keV −5% & +5%
ELEGP offset	^{123}I with ^{99m}Tc background	ELEGP	159 keV −5.5% & +15.5%
LEHR reference	^{123}I only	LEHR	159 keV −10% & +10%
LEHR normal	^{123}I with ^{99m}Tc background	LEHR	159 keV −10% & +10%
LEHR narrow	^{123}I with ^{99m}Tc background	LEHR	159 keV −5% & +5%
LEHR offset	^{123}I with ^{99m}Tc background	LEHR	159 keV −5.5% & +15.5%

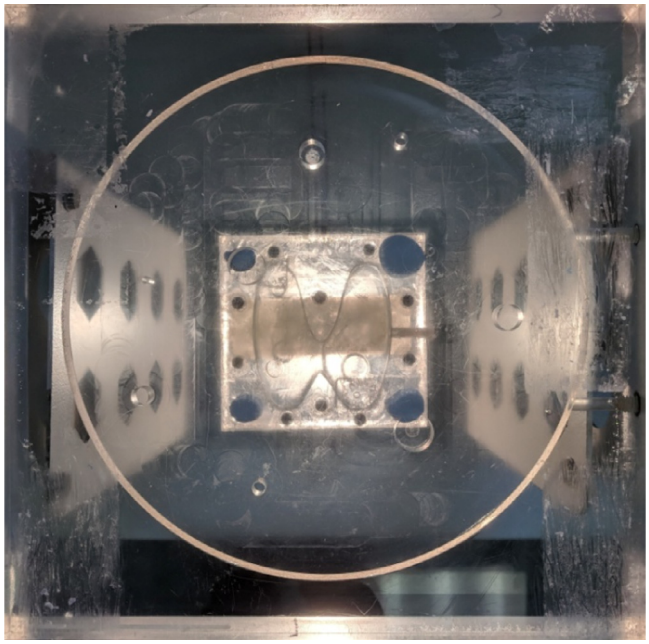

Fig. 3. Phantom and shell setup used for planar acquisitions.

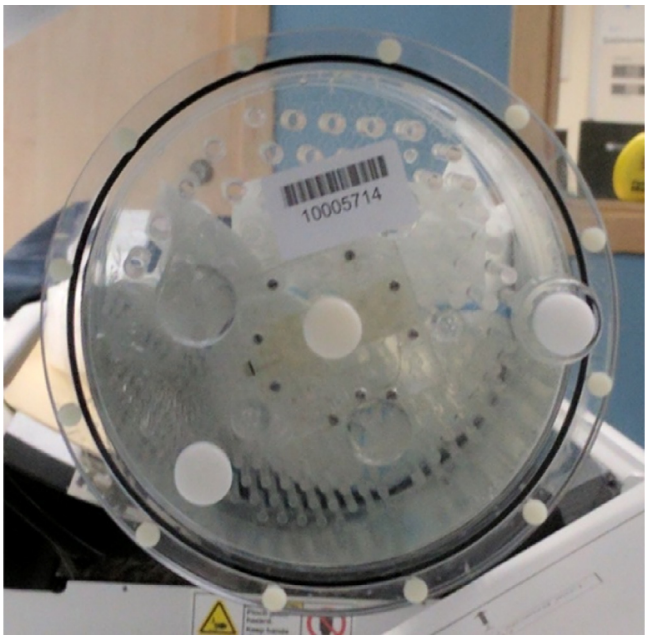

Fig. 4. Striatum mimic phantom setup used for SPECT acquisitions.

amount of activity was determined to give approximately the same count rate as seen on a typical clinical patient.

A bespoke Perspex "shell phantom" was positioned on top (Fig. 3). This phantom contained a cylindrical cavity with a volume of 300 mL situated inside a cuboid. Initially the shell was filled with water to simulate ^{123}I only acquisitions. For the simultaneous protocol 47 kBq/mL of ^{99m}Tc was added for the remaining acquisitions; again this amount of activity was determined to give the equivalent count rate as seen on a typical clinical patient. In total eight planar images were acquired (Table 1).

For the delay protocol the above set of acquisitions was repeated with 30 kBq/mL of ^{99m}Tc instead of 47 kBq/mL to simulate a four hour delay between acquisitions. This is a suitable method to simulate the delay as it is known that little ^{99m}Tc activity is lost from the cerebrum in the 24 h after initial washout except by radioactive decay [8].

Images were analysed on a Xeleris 3 workstation (GE Healthcare, Waukesha, WI, USA). Circular regions of interest (ROIs) with a diameter of 1 cm were centered on the cold (no activity) and hot (high activity) regions as indicated by the schematic (Fig. 2). Two background ROIs of the same size and shape were placed in the background. Contrast to Noise ratios (CNRs) were calculated for each region using Eq. (1) as defined by Cherry et al. [9].

$$CNR = \frac{|ROI - Bkg|}{Bkg} \times d_l \times \sqrt{\frac{Bkg}{ROI_{Area}}} \quad (1)$$

Where ROI is the average count in either the cold or hot region, Bkg is the average count in the corresponding background region, d_l is the diameter of the ROI and ROI_{Area} is the area of the ROI.

Planar ^{123}I spatial resolution was measured by filling a glass capillary tube with ^{123}I sodium iodide. The capillary was positioned centrally in parallel with the y-axis. The shell phantom was prepared as detailed above for the planar images. This phantom was then positioned on top of the capillary tube. Images were acquired using the same parameters as detailed above for the planar acquisitions. x-axis line profiles were extracted from the images along the length of the tube. The FWHM of these profiles was used to determine the spatial resolution for each acquisition method. The error in this measurement was estimated as half the pixel size (1.1 mm)

2.2. SPECT

SPECT images were acquired using 128 × 128 matrix, 60 dual-head positions at a radius of 15 cm over an 180° circular orbit resulting in 120 projections covering 360°. Step and shoot mode was used with an acquisition time of 30 s per projection. A zoom factor of 1.14 was applied and only LEHR collimators were used. These parameters are the same as the clinical setup.

The striatum mimic phantom was filled as before for the planar acquisitions and then placed inside a Perspex cylinder filled with water (Fig. 4). The phantom was positioned in the centre of the FOV using a jig. After the first acquisition (Table 2), 9 MBq ^{99m}Tc was added to the volume of the cylinder and the remaining acquisition was taken using the jig to ensure the positioning was reproduced. Once again the activity used was chosen based on the activity that would replicate the count rates achieved clinically and then decayed for 4 h.

Table 2
Collimator and energy window combinations for SPECT acquisitions.

SPECT acquisition method	Phantom setup	Collimator	Energy window
Reference	^{123}I only	LEHR	159 keV −10% & +10%
Offset	^{123}I with ^{99m}Tc background	LEHR	159 keV −5.5% & +15.5%

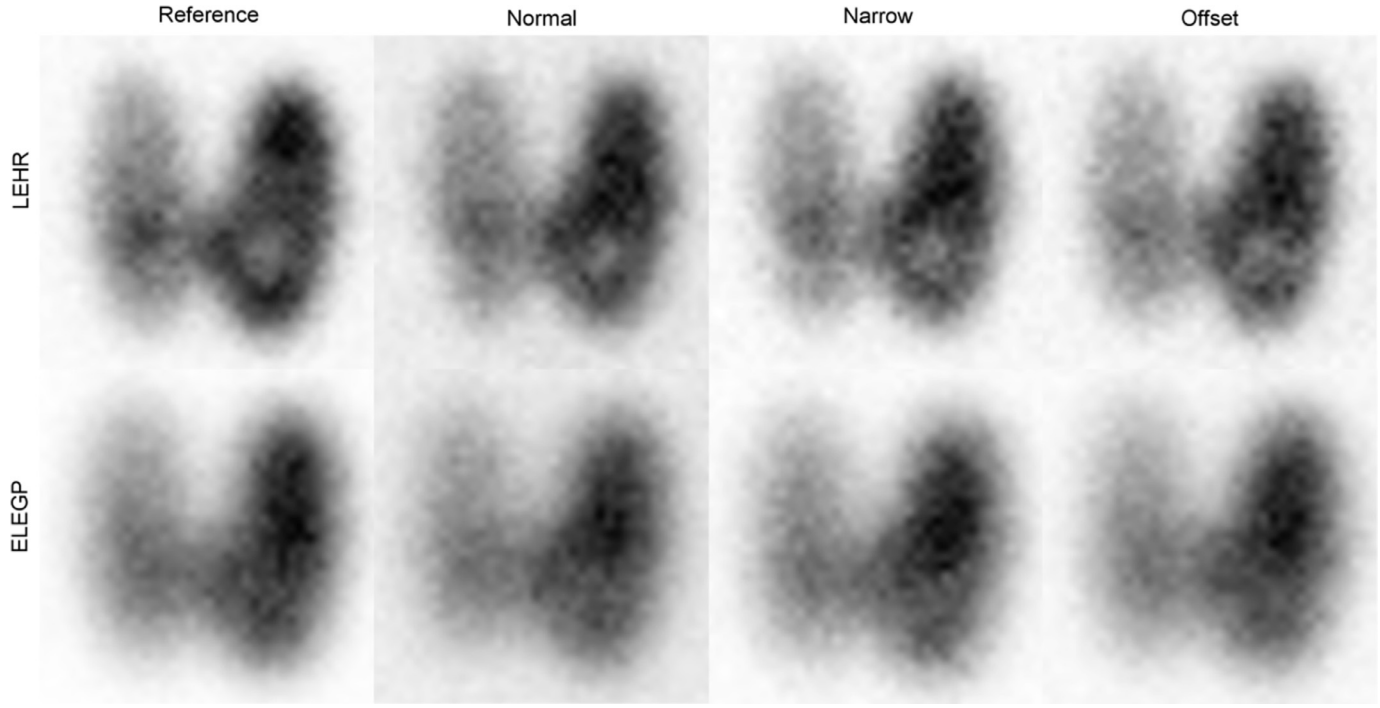

Fig. 5. Planar ^{123}I images for the different acquisition methods using the simultaneous protocol.

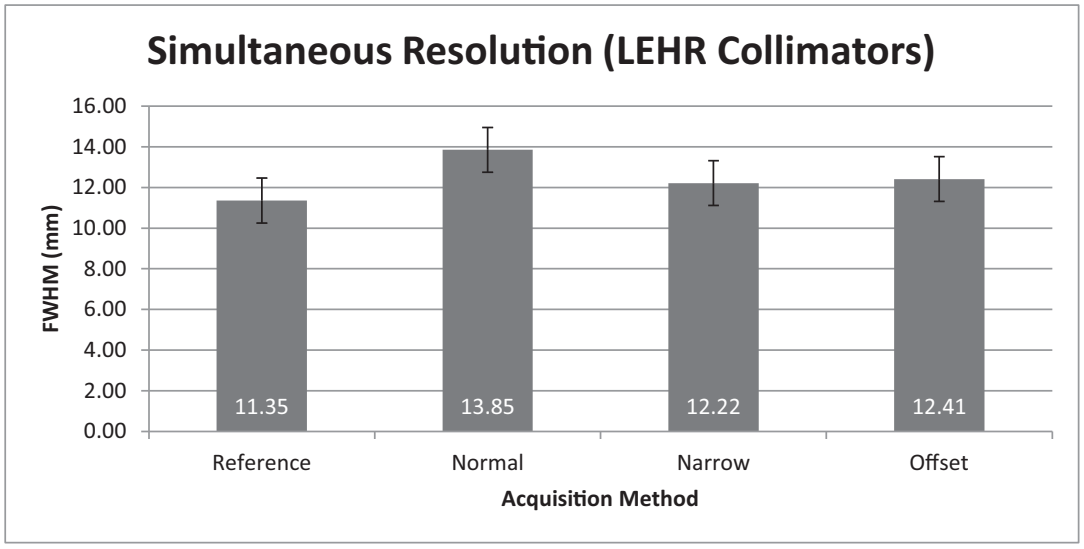

Fig. 6. Estimated planar spatial resolution for ^{123}I using each acquisition method assuming acquisition was at the same time.

SPECT images were reconstructed using an ordered subset expectation maximisation (OSEM) reconstruction algorithm (GE Xeleris 3 Workstation, 2 Iterations 10 Subsets Butterworth Filter Power 10 Cutoff 0.65 cycles/cm) with no corrections applied. These parameters follow the manufacturer's recommendations for the system used for this work. They were determined using data from a phantom acquisition and the same parameters are used clinically. Resolution recovery was used in addition to the above reconstruction parameters for both the reference and offset acquisitions.

3. Results

3.1. Simultaneous planar images

Looking at the ELEGP reference image (Fig. 5) it is evident that this collimator set was not able to provide the necessary resolution to resolve the hot and cold regions in the phantom.

The presence of ^{99m}Tc degraded the achievable spatial resolution (Fig. 6). Narrowing the energy window improved the resolution but not to the same level as the reference case. Using an offset

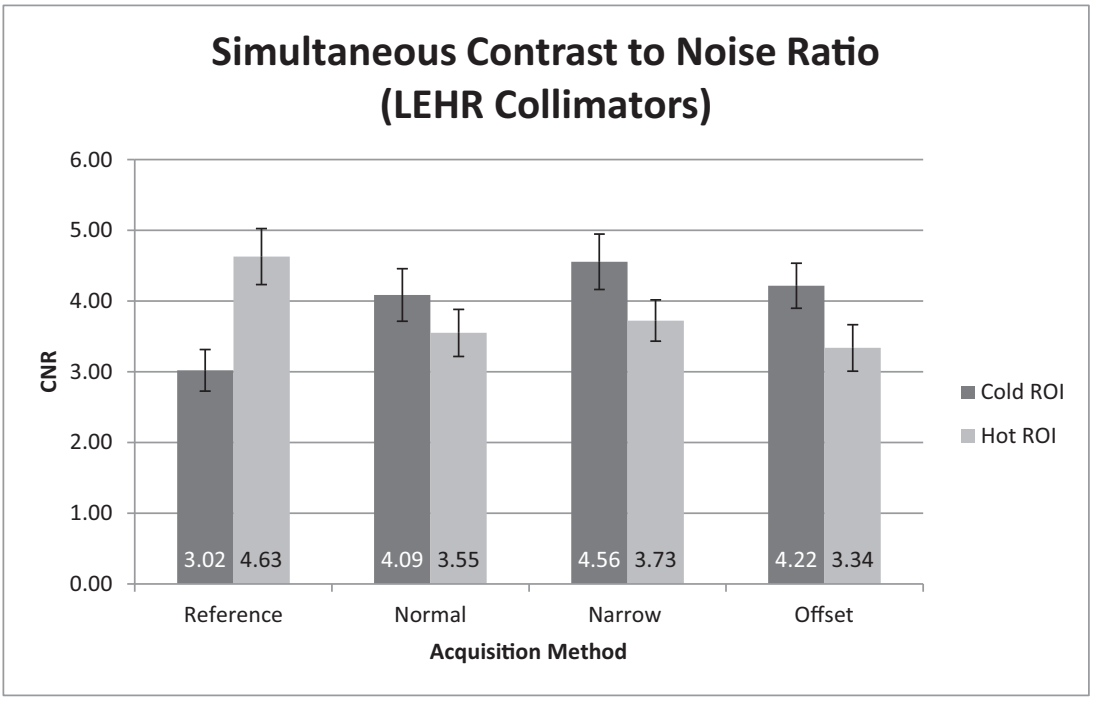

Fig. 7. Contrast to Noise Ratio (CNR) for the hot and cold regions of the phantom using the same time protocol.

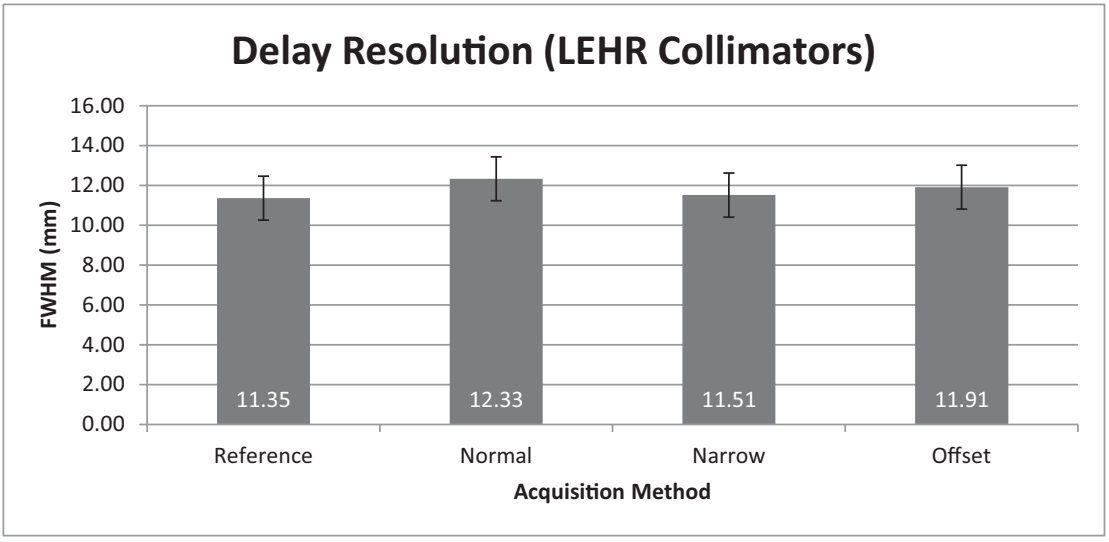

Fig. 8. Estimated planar spatial resolution for ^{123}I using each acquisition method if acquisitions were on the same day with a four hour delay.

window also compensated for the degraded resolution but only by a similar amount to the narrow window.

CNR for the hot region was reduced with the introduction of ^{99m}Tc (Fig. 7) and this can be seen visually in the images themselves (Fig. 5). The higher level of background counts caused by the ^{99m}Tc background has artificially increased the contrast of the cold spot. The level of noise (standard deviation of the background counts) is similar to the reference for the narrow and offset windows. This results in a higher cold CNR for the narrow and offset windows. There is an increased level of noise for the normal window which counteracts the artificial increase in contrast.

3.2. Delay planar images

The delay planar spatial resolution follows the same pattern as the simultaneous setup however the loss of resolution is less across all three acquisition methods (Fig. 8). The narrow energy window has a comparable level of resolution to the reference setup.

The results from the delay protocol given in Fig. 9 show that whilst a narrow window provided the best planar image resolution with the ^{99m}Tc background, the offset window provided a higher CNR for the hot ROI. The CNR value achieved using the offset window is comparable to the reference value. Again the ^{99m}Tc background has artificially increased the contrast of the cold spot however there is an increased level of noise for the normal and offset window (Fig. 10). The narrow window has a similar level of noise to the reference.

3.3. Delay SPECT images

The reconstructed offset window SPECT images are comparable to the reference SPECT images (Fig. 11). The resolution recovery

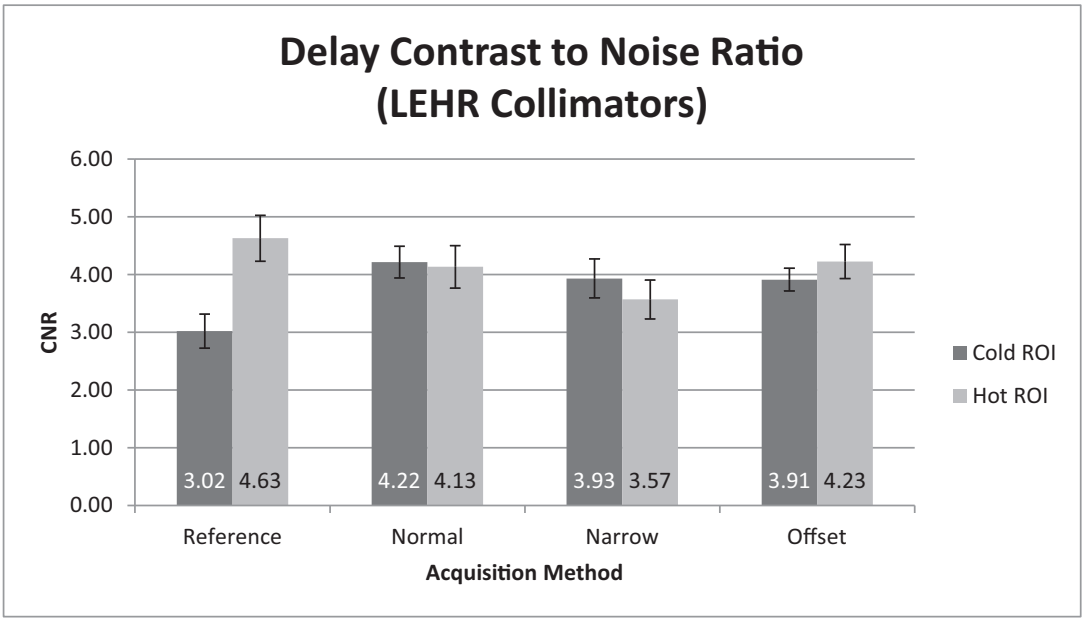

Fig. 9. Contrast to Noise Ratio (CNR) for the hot and cold regions of the phantom using the delay protocol.

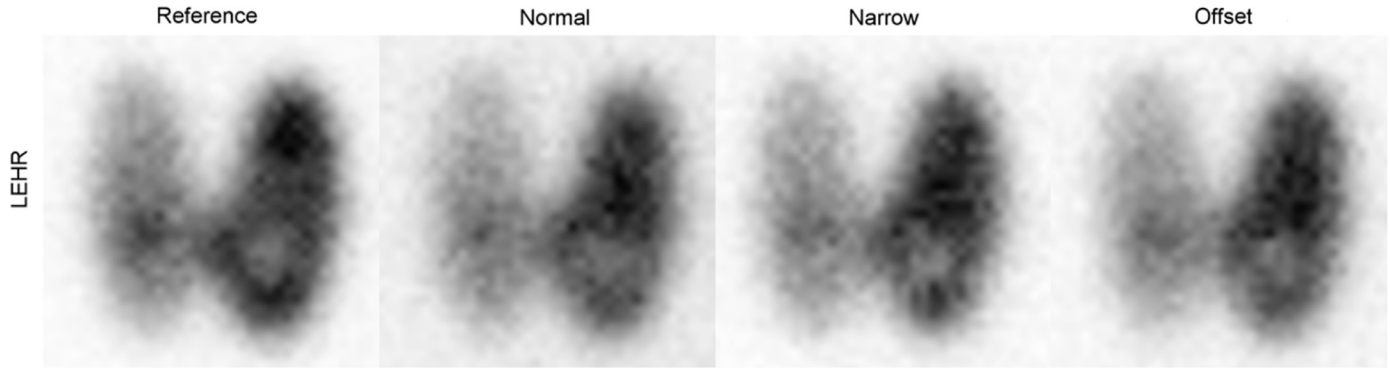

Fig. 10. Planar ^{123}I images for the different acquisition methods using the delay protocol.

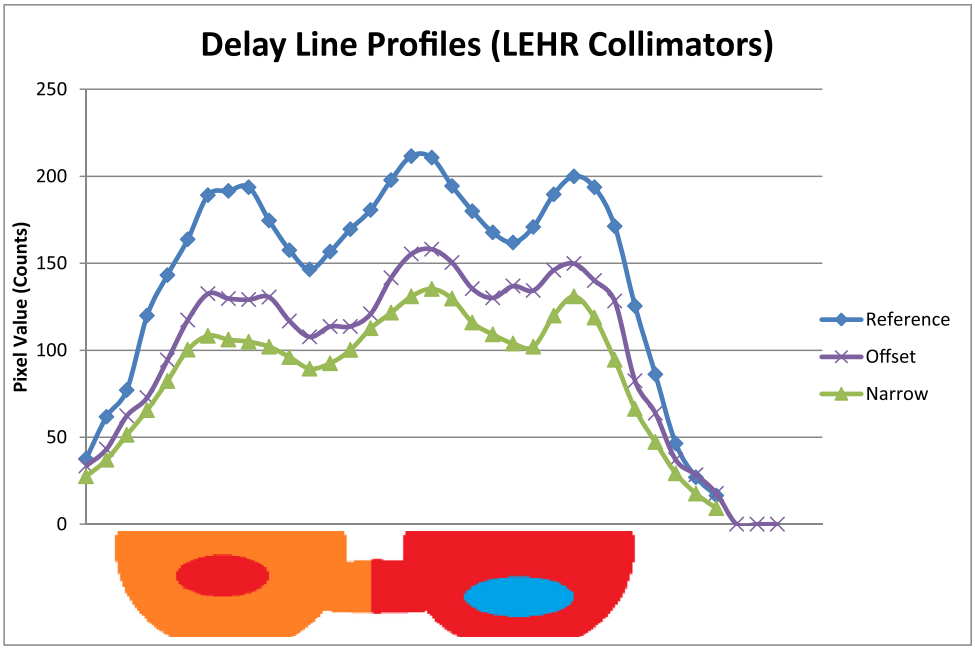

Fig. 11. Line profiles through the two ROIs for different acquisition methods using the delay protocol. The phantom schematic is aligned along the *x*-axis to indicate the true hot and cold regions.

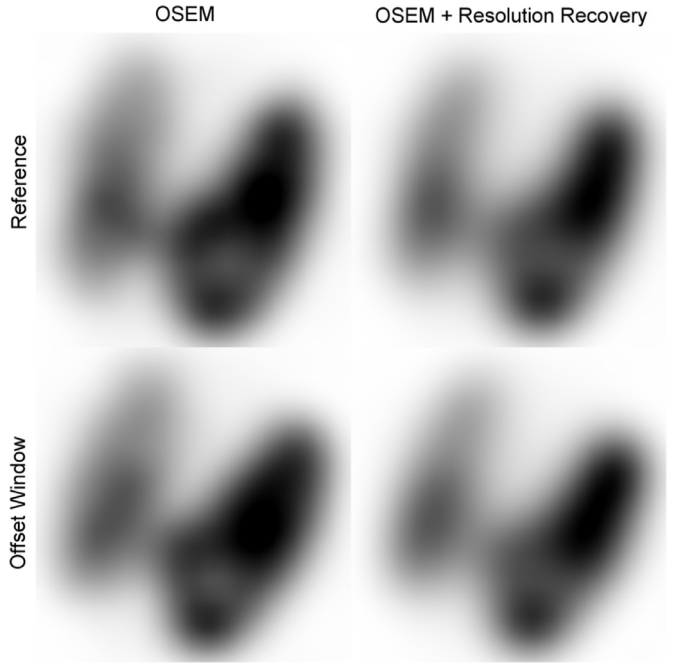

Fig. 12. Reconstructed SPECT images using an OSEM algorithm with and without resolution recovery using the delay protocol.

algorithm produces images that are smoother in appearance with higher CNR values for the Hot ROI (Fig. 12). However the CNR values for the cold ROI are slightly reduced (Fig. 13) and the shape of the cold ROI is distorted from its circular shape, with resolution recovery.

This change in the cold contrast is visualised very well by the two sets of line profiles. The cold region "dip" in the OSEM only profiles (Fig. 14) is missing entirely in the resolution recovery profiles (Fig. 15). It should be noted that this effect happens for both the reference and offset window.

4. Discussion

These initial phantom results show that a same day imaging protocol can achieve comparable levels of CNR with very small losses in image resolution. This suggests that diagnostic quality Ioflupane (^{123}I) SPECT images could be acquired on the same day as Exametazime (^{99m}Tc) SPECT using a different energy window and a four hour delay to compensate for ^{99m}Tc crosstalk.

While the results are encouraging this work was limited by the availability of phantoms. The phantoms used are of the correct order of magnitude in terms of size but they may not produce the same level of scatter as would be seen clinically. The study was designed to replicate a typical patient and consideration should be given to the worst case scenario where there is high uptake of ^{99m}Tc and low uptake of ^{123}I. While image quality is the most important factor there is an increasing amount of quantitation being carried out on Ioflupane (^{123}I) SPECT images [10]. Quantitation may be compromised by dual energy acquisitions.

Although ELEGP collimators are designed to accommodate the higher energy components of the ^{123}I spectrum they did not provide the necessary resolution to gain any meaningful results from this study. The low resolution would mean any small changes would be missed in clinical images.

Using the resolution recovery algorithm improved the contrast of the hot region however the images looked qualitatively smoother in appearance. The use of the resolution recovery algorithm causes a decrease in the contrast of the cold region and a visual distortion of the cold ROI from its circular shape.

Other crosstalk compensation techniques can be found in the literature and these techniques may be able to further improve image quality [4–6]. However as mentioned previously these techniques can be complex and time consuming to implement.

Solid state gamma cameras are now available on the market. These cameras are capable of achieving an energy resolution of approximately 6.3%. In practical terms this energy resolution would reduce the width of the detected energy spectrums which in turn reduces the amount of crosstalk which is the fundamental challenge in dual-isotope imaging.

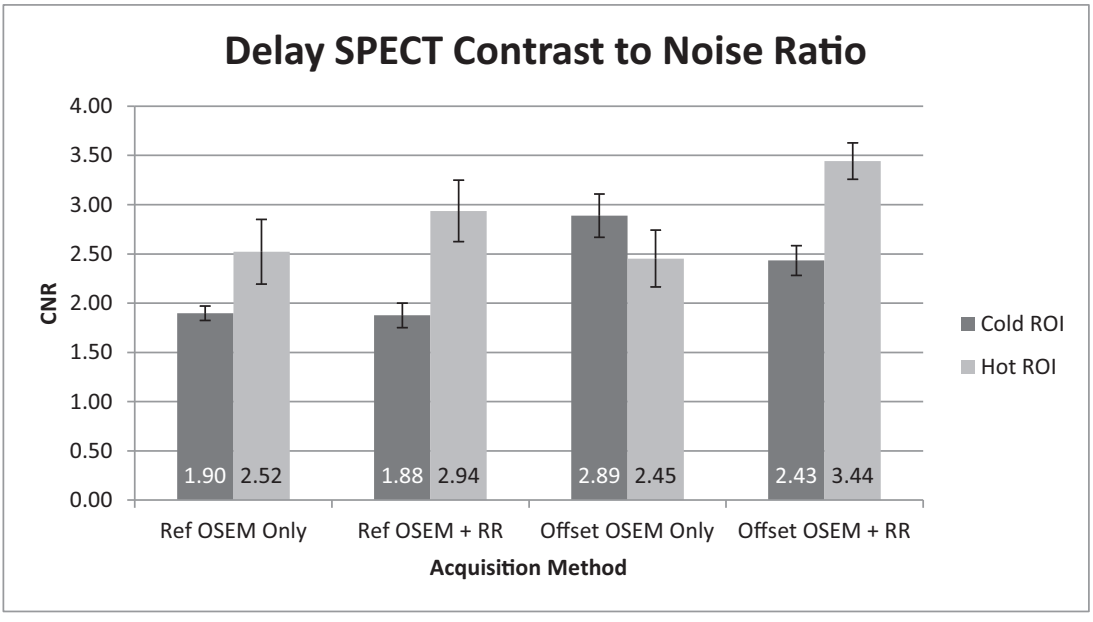

Fig. 13. Contrast to Noise Ratio (CNR) for the hot and cold regions of the phantom in the SPECT images using the delay protocol.

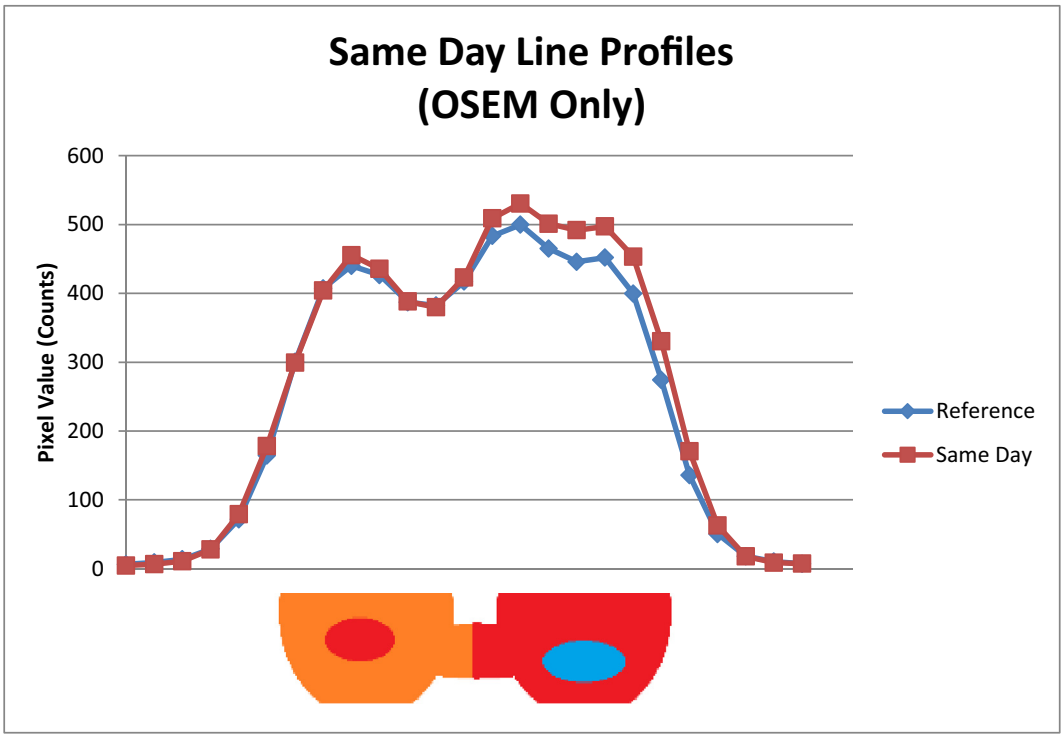

Fig. 14. Line profiles through the two ROIs for the reference and offset energy window acquisitions. The phantom schematic is aligned along the *x*-axis to indicate the true hot and cold regions.

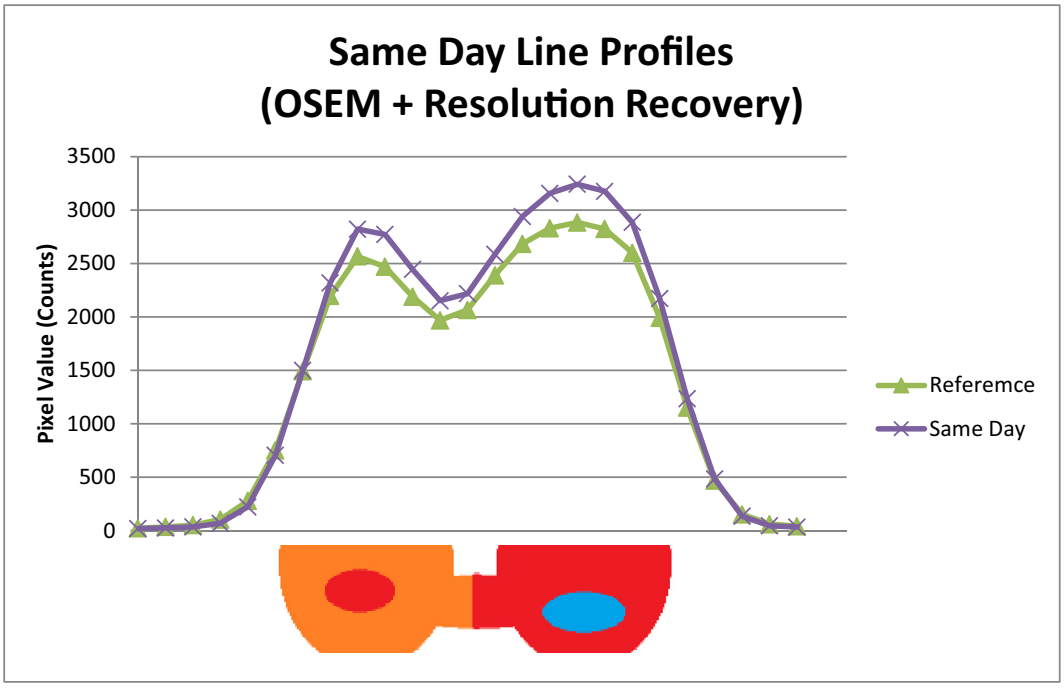

Fig. 15. Line profiles through the two ROIs for the reference and offset energy window acquisitions using resolution recovery in the reconstruction. The phantom schematic is aligned along the *x*-axis to indicate the true hot and cold regions.

This work has provided a fundamental proof of concept for same day imaging. Image quality may be compromised to a small extent and this degradation must be balanced by the benefit of imaging on the same day.

Conflict interest

None.

Sources of funding

No specific funding was obtained for this work.

Ethical approval

N/A.

Acknowledgments

The author has no competing interests and no specific funding was obtained for this work. The author would like to thank the technical and scientific staff in Nuclear Medicine at Ninewells Hospital, Dundee for all of their help with this work.

References

[1] Samii A, Nutt JG, Ransom BR. Parkinson's disease. Lancet 2004;363:1783–93.
[2] Van Laere K, Casteels C, De Ceuninck L, Vanbilloen B, Maes A, Mortelmans L, Vandenberghe W, Verbruggen A, Dom R. Dual-tracer dopamine transporter and perfusion SPECT in differential diagnosis of parkinsonism using template-based discriminant analysis. J Nucl Med 2006;47(3):384–92.
[3] Devous MD, Lowe JL, Payne JK. Dual-isotope brain SPECT imaging with Technetium and Iodine-123: validation by Phantom studies. J Nucl Med 1992;33(11):2030–5.
[4] El Fakhri G, Maksud P, Kijewski MF, Zimmerman RE, Moore SC. Quantitative simultaneous 99mTc/123I SPECT: design study and validation with Monte Carlo simulations and physical acquisitions. IEEE Trans Nucl Sci 2002;49(5):2315–21.
[5] Du Y, Tsui BM, Frey EC. Model-based crosstalk compensation for simultaneous 99mTc/123I dual-isotope brain SPECT imaging. Med Phys 2007;34(9):3530–43.
[6] Chang C-J, Huang W-S, Su K-H, Chen J-C. Seperation of two Radionuclides in simultaneous dual-isopte imaging with independent component analysis. Biomed Eng- Appl Basis Commun 2006;18(5):264–9.
[7] Administration of Radioactive Substances Advisory Committee. Notes for guidance on the clinical administration of radiopharmaceuticals and use of sealed radioactive sources. Didcot: Public Health England; 2018.
[8] Healthcare GE. Ceretec-Kit for the preparation of technetium Tc99m exametazime injection. GE Healthcare, Arlington Heights; 2013.
[9] Cherry SR, Sorenson JA, Phelps ME. Physics in nuclear medicine. Philadelphia: Elsevier; 2012.
[10] Shimizu S, Namioka N, Hirose D, Kanetaka H, Hirao K, Hatanaka H, Takenoshita N, Kaneko Y, Ogawa Y, Tsugawa A, Umahara T, Sakurai H, Hanyu H. Comparison of diagnostic utility of semi-quantitative analysis for DAT-SPECT for distingushing DLB from AD. J Nucl Med 2017;377:50–4.